

Brain cortex mitochondrial bioenergetics in synaptosomes and non-synaptic mitochondria during aging

Silvia Lores-Arnaiz¹ · Paulina Lombardi¹ · Analía G. Karadayian¹ · Federico Orgambide¹ · Daniela Cicerchia¹ · Juanita Bustamante²

Received: 11 September 2015 / Revised: 23 December 2015 / Accepted: 25 December 2015 / Published online: 28 January 2016
© Springer Science+Business Media New York 2016

Abstract Alterations in mitochondrial bioenergetics have been associated with brain aging. In order to evaluate the susceptibility of brain cortex synaptosomes and non-synaptic mitochondria to aging-dependent dysfunction, male Swiss mice of 3 or 17 months old were used. Mitochondrial function was evaluated by oxygen consumption, mitochondrial membrane potential and respiratory complexes activity, together with UCP-2 protein expression. Basal respiration and respiration driving proton leak were decreased by 26 and 33 % in synaptosomes from 17-months old mice, but spare respiratory capacity was not modified by aging. Succinate supported state 3 respiratory rate was decreased by 45 % in brain cortex non-synaptic mitochondria from 17-month-old mice, as compared with young animals, but respiratory control was not affected. Synaptosomal mitochondria would be susceptible to undergo calcium-induced depolarization in 17 months-old mice, while non-synaptic mitochondria would not be affected by calcium overload. UCP-2 was significantly up-regulated in both synaptosomal and submitochondrial membranes from 17-months old mice, compared to young animals. UCP-2 upregulation seems to be a possible mechanism by which mitochondria would be resistant to suffer oxidative damage during aging.

Keywords Synaptosomes · Non-synaptic mitochondria · Aging · Cerebral cortex · Respiration · Depolarization

Abbreviations

CNS	Central nervous system
COX	Cytochrome c oxidase
EDTA	Ethylenediaminetetraacetic acid
FCCP	Carbonyl cyanide p-trifluoromethoxyphenylhydrazone
FSC	Forward side scatter
MPT	Mitochondrial permeability transition
NMDA	<i>N</i> -methyl-D-aspartate
RCR	Respiratory control rate
ROS	Reactive oxygen species
SSC	Side scatter
TMRE	Tetramethylrhodamineethyl ester
UCP	Uncoupling protein
VDAC	Voltage-dependent anion channel

Introduction

Mitochondria present at the presynaptic terminals are capable of producing most of the ATP required to maintain ion homeostasis and phosphorylation reactions [1].

At the postsynaptic level, a high amount of energy production is required, mainly for reversing ion influxes underlying action potential signaling [2]. Additionally, at the pre-synaptic terminals, energy is also required for vesicle trafficking and neurotransmitters pumping into synaptic vesicles [3].

Mitochondria have the ability to buffer cytoplasmic Ca^{2+} ; their localization in neurons can therefore influence local regulation of Ca^{2+} -mediated synaptic plasticity [4, 5]. The presence and correct functioning of mitochondria at synapses with high energy and Ca^{2+} -buffering demands is

✉ Silvia Lores-Arnaiz
slarnaiz@ffyb.uba.ar

¹ Instituto de Bioquímica y Medicina Molecular, Facultad de Farmacia y Bioquímica, Universidad de Buenos Aires, Junín 956, C1113AAD, Buenos Aires, Argentina

² Centro de Altos Estudios en Ciencias de la Salud, Universidad Abierta Interamericana, Buenos Aires, Argentina

necessary for a proper neuronal function [6, 7]. In addition, mitochondrial swelling can block the axonal trafficking, contributing to neuronal metabolic disruption [8]. Impairment of the synaptic function in neurodegenerative disease has been associated with disruption of mitochondrial trafficking, distribution and function [9].

Synaptosomal subcellular preparations provide an accurate model to test mitochondrial function in the nervous system [10]. Mitochondria inside the synaptosomes supply ATP to the cytoplasm and plasma membrane and preserve metabolism, plasma membrane excitability, receptors and ion channels functioning and machinery for the exocytosis and reuptake of neurotransmitters [11]. Synaptosomes are accessible to many of the techniques employed for the evaluation of bioenergetic parameters including mitochondrial membrane potential and respiratory rates, as well as mitochondrial Ca^{2+} uptake [11]. Regarding calcium homeostasis, Brown et al. [12] have shown that rat cortex non-synaptic mitochondria can accumulate significantly more Ca^{2+} than the synaptic mitochondria before undergoing MPT.

The aging process has been associated with a reduction in the bioenergetic capacity, increased active oxygen species generation and impairment of calcium homeostasis.

Mitochondria are considered the main intracellular source of oxygen free radicals generation and also the main target of free radicals-mediated damage. Accumulation of oxygen radicals-induced oxidative damage during aging leads to significant changes in brain mitochondrial function [13]. It has been previously established that during aging and neurodegenerative diseases, dysfunctional synaptic mitochondria might not satisfy the high energy demands required at the synapses leading to impaired neurotransmission and cognitive failure [14].

Recent studies from our laboratory have shown that synaptic mitochondria seem to be more susceptible than non-synaptic mitochondria to suffer mitochondrial respiratory dysfunction and alterations in calcium homeostasis in 14-months old animals [15].

The aim of this study was to evaluate alterations in mitochondrial function in synaptosomes and non-synaptic mitochondria obtained from 3- and 17-months old mice. Mitochondrial physiology will be analyzed by respiratory rate measurements, mitochondrial membrane potential response to calcium insult, activity of mitochondrial respiratory complexes and UCP-2 expression.

Materials and methods

Animals

Male Swiss mice of 3 or 17 months old were used. All efforts were made to minimize animal discomfort and to

reduce the number of animals used. Animal handling and treatment, as well as all experimental procedures were reviewed in accordance with the guidelines of the National Institute of Health (USA), and with the 6344/96 regulation of the Argentinean National Drug Food and Medical Technology Administration. Moreover, the present study had the legal ethical accreditation from Ethics Committee for Laboratory Animal Handling of the School of Pharmacy and Biochemistry from Universidad de Buenos Aires where the protocol was performed.

Isolation of subcellular fractions

Animals were killed by decapitation and the brains were immediately excised. Brains were weighed, cerebral cortex was dissected and homogenized in a medium consisting of 0.23 M mannitol, 0.07 M sucrose, 5 mM HEPES and 1 mM EDTA (MSHE), pH 7.4, and homogenized at a ratio of 1 g brain/5 ml homogenization medium. Homogenates were centrifuged at 600 g for 10 min to discard nuclei and cell debris and the supernatant was centrifuged at 8000 g for 10 min. The resulting pellet was washed and resuspended in the same buffer.

Further mitochondrial purification and synaptosomal fraction separation were performed by Ficoll gradient [16] with modifications. The crude mitochondrial fraction was resuspended in MSHE buffer and layered on Ficoll gradients containing steps of 13, 8 and 3 % Ficoll [17]. The gradients were centrifuged at 11,500 g for 30 min. After centrifugation, the original sample appears separated in two fractions: a pellet in the bottom of the tube corresponds to a fraction of heavy mitochondria, which are mainly non-synaptic and the fraction occurring at 8 % contains synaptosomes. All the procedure was carried out at 0–2 °C. Submitochondrial membranes were obtained from mitochondria by twice freezing, thawing and homogenizing by passing the suspension through a 15/10 hypodermic needle [18]. Protein content was assayed by using the Folin phenol reagent and bovine serum albumin as standard [19].

The operations were carried out at 0–2 °C. Mitochondrial yield was estimated in approximately 30–45 mg mitochondrial protein/g brain tissue, both for non-synaptic and synaptosomal fraction. This estimation was based on the determination of the activity of monoamine oxidase both in total homogenates and in mitochondrial or synaptosomal fractions. Non-synaptic mitochondria were less than 5 % contaminated with synaptosomal components, according to acetylcholinesterase activity determinations [15].

Mitochondrial respiration

A two-channel respirometer for high-resolution respirometry (Oroboros Oxygraph, Paar KG, Graz, Austria) was

used. Oxygen consumption rate of intrasynaptosomal mitochondria was determined in synaptosomal fractions from 3 or 17 months-old mice. The reaction medium consisted of 120 mM NaCl, 3.5 mM KCl, 1.3 mM CaCl₂, 0.4 mM KH₂PO₄, 15 mM D-glucose, 10 mM pyruvate, 0.4 % (w/v) fatty acid-free bovine serum albumin and 10 mM HEPES, pH 7.4. The addition of a high Ca²⁺ concentration is supposed to damage mitochondria outside the synaptosomes but does not harm real synaptic mitochondria localized inside synaptosomes, allowing the measurement of oxygen uptake only from synaptosomes. Maximal respiration was achieved after addition of 4 μM FCCP; respiration driving proton leak was determined after addition of 4 μg/ml oligomycin, an inhibitor of ATP synthase; respiration driving ATP synthesis was calculated as the basal respiration minus respiration driving proton leak and spare respiratory capacity was estimated as a percentage ratio between maximum and basal respiration [20].

In non-synaptic mitochondria from 3 or 17 months-old animals, mitochondrial respiratory rates were measured in a reaction medium containing 0.23 M mannitol, 0.07 M sucrose, 20 mM Tris-HCl (pH 7.4), 1 mM EDTA, 4 mM MgCl₂, 5 mM phosphate and 0.2 % bovine serum albumin at 30 °C, using malate 6 mM and glutamate 6 mM or succinate 7 mM to measure state 4 respiration and adding 1 mM ADP to measure state 3 respiration. The respiratory control ratio (state 3 respiration/state 4 respiration) was determined [21].

Flow cytometry analysis

Flow cytometry analysis was performed based on Forward angle light scatter (FSC) which is proportional to particle size, and wide angle or side scatter (SSC) scatter that gives information about relative granularity or internal complexity. The light scattering properties of the synaptosomal and mitochondrial fractions were determined in comparison with size standards indicating that particles range in size from less than 1 μm to more than 6 μm (data not shown). Synaptosomes are among the largest particles in a crude synaptosomal preparation, while the major contaminants known to be present are small structures and include free mitochondria, myelin, lysosomes, and membrane fragments. In addition, immediately after isolation, the two subcellular fractions (synaptosomes and non-synaptic mitochondria) were routinely stained with the fluorophore 10 N-nonylacridine orange (NAO), in order to detect mitochondrial positive particles by flow cytometry. This fluorescent dye binds tightly to the acidic phospholipid cardiolipin, which is found exclusively in mitochondrial and bacterial membranes [22]. Both subcellular fractions analyzed showed 65 % of NAO-positive particles, revealing the presence of mitochondria either free or inside the synaptosomes.

The analysis by flow cytometry parameters presents several advantages as stated by Choi et al. [20]. This method enables the selection of synaptosomal particles by SSC and FSC parameters for data analysis, by excluding extraneous objects such as broken synaptosomes or non-synaptic material. This last advantage is particularly important in experiments using synaptosomes because these preparations also contain broken membranes and empty synaptosomes, visible by electron microscopy, that do not interfere with the entrapped fluorescence probe methods used in this assay.

Mitochondrial membrane potential

Mitochondrial transmembrane potential was determined as follows: isolated synaptosomes or non-synaptic mitochondria (25 μg/ml) were incubated at 37 °C for 20 min in MSH buffer supplemented with 5 mM malate, 5 mM glutamate, 1 mM phosphate and 4 mM MgCl₂ in the presence of 500 nM TMRE, a potentiometric probe that can be used for direct measurement of trans-membrane potential in cells and isolated mitochondria from different sources. The fluorescence changes were determined by cytometric measurements. Fresh samples were prepared for each experiment and were protected from light until acquired by the cytometer. Auto-fluorescence of the preparations was measured as a probe loading control, and 0.5 μM of the depolarizing agent FCCP was used as a positive control [23]. Histogram differences in TMRE fluorescence were quantified in three independent experiments as the number of events which drop under the median value of the distribution using a common marker (M1). A higher amount of events with low fluorescence would reflect mitochondrial membrane depolarization. Quantification of results was shown as bar graph in which data were expressed as the percentage of control of TMRE fluorescence. The RCR was not affected by the concentration of the potentiometric probe used.

Evaluation of respiratory complexes activity

NADH-cytochrome *c* reductase activity (complex I + III) was measured in the two subcellular fractions by following spectrophotometrically the reduction of cytochrome *c* at 30 °C at 550 nm ($\epsilon = 19.6 \text{ mM}^{-1} \text{ cm}^{-1}$) in a reaction medium containing 100 mM phosphate buffer (pH 7.4), 0.2 mM NADH, 0.1 mM cytochrome *c* and 0.5 mM KCN. Enzyme activity was expressed in nmoles cytochrome *c* reduced per minute per mg of protein. Succinate cytochrome *c* reductase activity (complex II + III) was similarly determined and expressed, except that NADH was substituted by 20 mM succinate. Cytochrome oxidase activity (complex IV) was assayed spectrophotometrically at 550 nm by following the rate of oxidation of 50 μM

ferrocytochrome *c* [24]. The activity was expressed as nmoles ferrocytochrome *c* oxidized per minute per mg of protein.

UCP-2 expression

Uncoupling proteins (UCP) are a heterogeneous family of proteins that play an important role in partially dissipating the proton electrochemical gradient across the inner mitochondrial membrane and uncoupling respiratory chain function from ATP synthesis [25]. Expression of UCP-2 isoform was analyzed by Western blot. Samples were obtained in the presence of protease inhibitors (1 µg/ml pepstatin, 1 µg/ml leupeptin, 0.4 mM phenylmethylsulfonyl fluoride and 1 µg/ml aprotinin). Submitochondrial membranes (80 µg) were separated by SDS-PAGE (12 %), blotted onto a nitrocellulose membrane (Bio-Rad, München, Germany) and probed primarily with rabbit polyclonal antibodies (dilution 1:500) to UCP-2 residue C-terminal (ABCAM Inc., USA). Then, the nitrocellulose membrane was incubated with a secondary goat anti-rabbit antibody conjugated with horseradish peroxidase (dilution 1:5000), followed by development of chemiluminescence with the ECL reagent (Santa Cruz Biotechnology) for 2–4 min. Voltage-dependent anion channel (VDAC) was used as loading control. Densitometric analysis of UCP-2 and VDAC bands was evaluated through NIH Image J 1.47b software and expressed as the ratio of UCP-2/VDAC. All experiments were performed in triplicate.

Drugs and chemicals

ADP, antimycin, CaCl₂, Catalase, Cytochrome *c*, EDTA, FCCP, Folin reagent, free fatty acid BSA, Glutamic Acid, Hepes, KCN, Malic Acid, Mannitol, MgCl₂, NADH, NaN₃, SDS, Succinate, Sucrose, Trizma Base and Tween were purchased from Sigma Chemical Co. (St. Louis, Missouri). UCP-2 antibody was purchased from Abcam Inc., Cambridge, USA. Other reagents were of analytical grade. Goat VDAC antibody was obtained from Molecular Probes Inc, USA. APS, 2-mercaptoethanol, bisacrylamide, Laemmli Buffer, TEMED were acquired from Bio Rad (Laboratories Inc, Research Foundation, Oklahoma, USA). Other reagents were of analytical grade.

Statistics

Results are expressed as mean values ± SEM. Data were evaluated for normality distribution by Kolmogorov–Smirnov test in order to follow a posterior parametric or nonparametric statistical testing. The analysis of the results was performed using unpaired Student *t* test or ANOVA followed by post hoc Tukey tests in order to analyze if

differences between groups were significant. Graph Pad InStat software was used and a difference was considered to be statistically significant when $p < 0.05$.

Results

Mitochondrial respiration

Mitochondrial respiration was determined in synaptosomes and non-synaptic mitochondria from 3 or 17-months old mice by different experimental approaches.

Oxygen consumption rates for brain cortex synaptosomes are shown in Table 1. Significant decrements were observed in basal respiration (26 %) and respiration driving proton leak (33 %) in synaptosomes from 17-months old mice. Even when spare respiratory capacity was not modified by aging, a tendency to decrease was found in respiration driving ATP synthesis and in maximal respiration in aged mice.

Oxygen consumption rates for brain cortex non-synaptic mitochondria are shown in Table 2. When we evaluated malate-glutamate dependent respiratory rates, no differences were observed in oxygen consumption rates in non-synaptic mitochondria between 3 and 17 months old mice. When we used succinate as substrate, state 3 respiratory rate was decreased by 45 % in brain cortex non-synaptic mitochondria from 17-month-old mice, as compared with young animals, but respiratory control was not affected.

Flow cytometry analysis

The characterization of synaptosomal particles was performed by drawing a data analysis gate on forward scatter to measure markers of interest for viable mitochondria such as cardiolipin and voltage gradient positive particles in a selected size range [26]. The results showed that synaptosomes are among the largest particles in the crude synaptosomal preparation from young (Fig. 1a, b) as well as from old (Fig. 2a, b) mice. Figures 1c and 2c show fluorescence histograms illustrating specific NAO labeling of the smallest particles (R2) in the preparation, while the largest particles (R1) in the preparation are shown in Figs. 1d and 2d. The size standards calibration indicates that these particles were around 6 µm in diameter. Comparison of the NAO histograms for the synaptosomal preparations from young and old mice reveals that the fluorescence % intensity in the larger particles is much greater (99 and 98 % respectively) than in the smallest particles (2.5 and 1 % respectively). Similar analysis was performed for TMRE labeling in synaptosomal preparations from young and old mice, indicating as well that the fluorescence % intensity in the larger particles is much greater (99 and 98 % respectively) than in the smallest particles (17 and 2.8 % respectively) (Figs. 1e, 2e, 1f, 2f).

Table 1 Respiration rate parameters of brain cortex synaptosomal fractions from 3- or 17-months old animals

	Age	
	3-month	17-month
Basal respiration (ng at O/min.mg protein)	69.9 ± 6.5	51.4 ± 2.2*
Respiration driving ATP synthesis (ng at O/min.mg protein)	12.7 ± 0.7	9.4 ± 0.3
Respiration driving proton leak (ng at O/min.mg protein)	60.9 ± 5.8	40.6 ± 1.5*
Maximum respiration (ng at O/min.mg protein)	82.9 ± 7.1	67.1 ± 2.2
Spare respiratory capacity (%)	119.1 ± 4.9	130.8 ± 3.9

Values represent the mean ± SEM

Subcellular fractions were prepared from a pool of 4 mice cerebral cortexes. Assays were performed in three independent experiments

* $p < 0.05$, different from 3-month animals

Table 2 Malate-glutamate and succinate dependent oxygen consumption by brain cortex non-synaptic mitochondria from 3- or 17-months old animals

Substrates	Age (months)	O ₂ uptake (ng at O/min.mg protein)		
		State 4	State 3	RCR
Malate-glutamate	3	16 ± 2	57 ± 7	3.8 ± 0.6
	17	14 ± 3	40 ± 8	3.0 ± 0.1
Succinate	3	9 ± 1	38 ± 2	4.7 ± 0.8
	17	5 ± 1	21 ± 2*	4.2 ± 0.7

Values represent the mean ± SEM

Subcellular fractions were prepared from a pool of 4 mice cerebral cortexes. Assays were performed in three independent experiments

* $p < 0.05$, different from 3-month animals

Mitochondrial membrane potential

In this study, mitochondrial response to calcium-induced MPT was evaluated by mitochondrial membrane potential determinations.

Results of mitochondrial membrane potential determinations for synaptosomes and non-synaptic mitochondria are shown in Figs. 3 and 4, respectively. Specifically, Fig. 3 shows a typical experiment presenting the dot-blot of the synaptosomal population gated as R1 with specific SSC and FSC parameters, and the corresponding histograms for the different experimental conditions: control, Ca²⁺ and FCCP incubations of synaptosomes from 3 months (A) and from 17-months old mice (B). For each histogram, a common

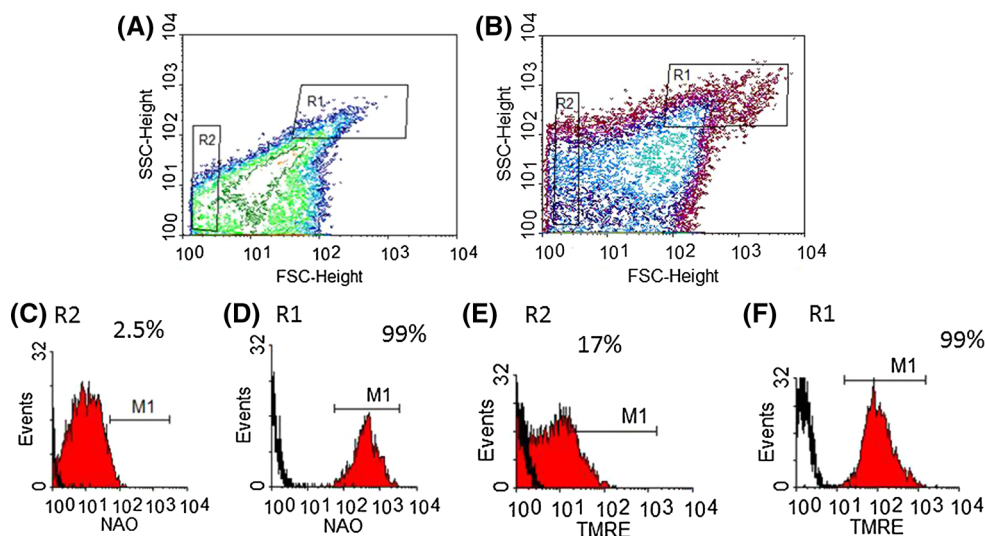


Fig. 1 Brain cortex synaptosomal fraction from young mice, labeled with NAO and TMRE. **a–b** Contour plot of forward angle scatter vs side angle scatter. Gates were drawn to include smallest particles (R2), and largest particles (R1). Both gates were drawn to include 20,000 particles. **c** and **e** Histogram plots of NAO and TMRE fluorescence falling within R2 (smallest particles). **d** and **f** Histogram

plots of NAO and TMRE fluorescence falling within R1 (largest particles). *Unshaded area* indicates autofluorescence, while shaded area indicates levels of NAO and TMRE fluorescence. *Marker 1* indicates the percentage of viable mitochondria inside the smallest and largest synaptosomal particles

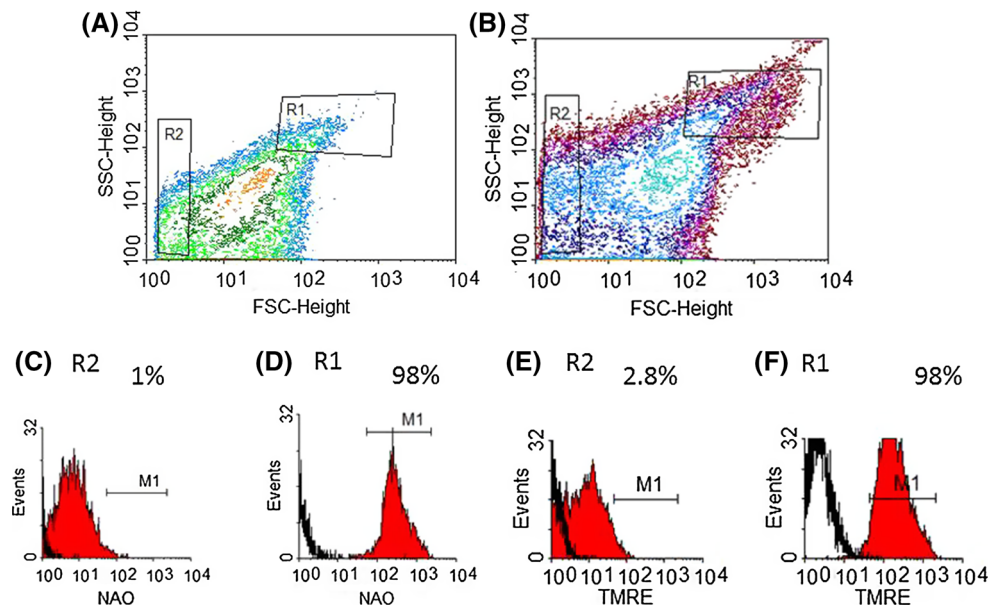


Fig. 2 Brain cortex synaptosomal fraction from old mice, labeled with NAO and TMRE. **a, b** Contour plot of forward angle scatter vs side angle scatter. Gates were drawn to include smallest particles (R2), and largest particles (R1). Both gates were drawn to include 20,000 particles. **c** and **e** Histogram plots of NAO and TMRE fluorescence falling within R2 (smallest particles). **d** and **f** Histogram

plots of NAO and TMRE fluorescence falling within R1 (largest particles). *Unshaded area*, indicates autofluorescence, while *shaded area* indicates levels of NAO and TMRE fluorescence. *Marker 1* indicates the percentage of viable mitochondria inside the smallest and largest synaptosomal particles

marker (M1) was set at the median value of the events of TMRE fluorescence and the corresponding percentage of events which drop under the median value was calculated. Autofluorescence corresponding to unloaded (no probe) synaptosomes are shown in the insets. Bar quantification of TMRE fluorescence for synaptosomes is shown in Fig. 3c. Mitochondrial membrane potential was not significantly affected by aging, but was decreased by 35 % by calcium addition in synaptosomes from 17-months old mice.

Mitochondrial membrane potential results obtained for non-synaptic mitochondria from 3 or 17-months old animals are shown in Fig. 4. Specifically, a typical experiment is presented, as described before, containing the dot-blot of the mitochondrial population and the gated R1 population with the histograms for the different conditions (control, Ca^{2+} and FCCP) corresponding to non-synaptic mitochondria from 3-months old (A) and 17-months old (B) animals. Bar quantification of TMRE fluorescence for non-synaptic mitochondria is shown in Fig. 4c. Mitochondrial membrane potential was not disturbed after 100 μM calcium incubation in either brain cortex non-synaptic mitochondria from young or old animals (Fig. 4c).

The mitochondrial uncoupler FCCP was used as positive control for mitochondrial depolarization. A significant mitochondrial depolarization (60–70 %) was observed after FCCP treatment both in synaptosomes (Fig. 3c) and non-synaptic mitochondria (Fig. 4c) of cerebral cortex from 3 or 17-months old animals.

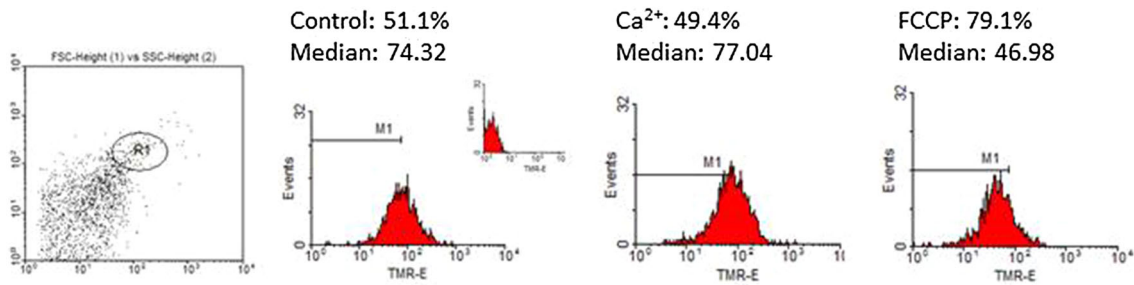
Respiratory complexes activity

Activity of complex I–III was not affected in synaptosomal membranes from 17-months old animals, but was significantly increased by 25 % in non-synaptic submitochondrial membranes from 17-months old animals, as compared with 3-months old mice (Table 3). Activity of complex II–III was 54 % increased in synaptosomes but remained unchanged in non-synaptic submitochondrial membranes in cerebral cortex from 17-months old animals (Table 3). Complex IV activity was increased in 17-months old animals both in cerebral cortex synaptosomes and in non-synaptic submitochondrial membranes by 63 and 38 % respectively (Table 3).

UCP-2 protein expression

UCP-2 protein expression was determined both in synaptosomal membranes and in submitochondrial membranes from 3 or 17-months old mice, by Western blot. Figure 5a shows Western blot analysis of UCP-2 protein expression in both subcellular fractions from 3- or 17-months old animals. VDAC was used as loading control. Results of the quantification of the UCP-2 and VDAC protein expression, obtained after densitometric analysis showed that the ratio of UCP-2/VDAC protein expression was 61 and 171 % increased in synaptosomal and submitochondrial membranes from 17-months old mice, as compared with young animals (Fig. 5b).

(A) Synaptosomes 3 months



(B) Synaptosomes 17 months

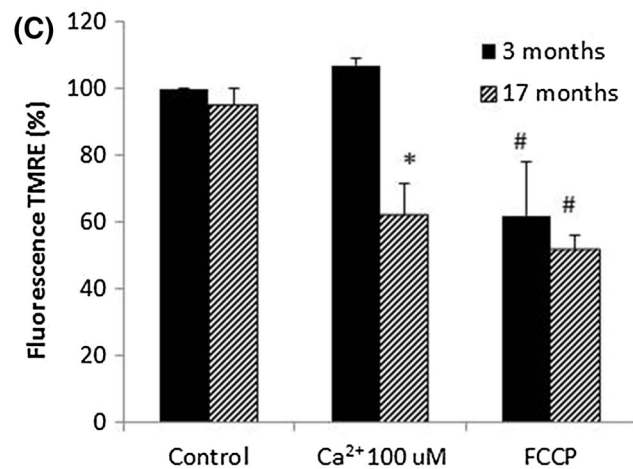
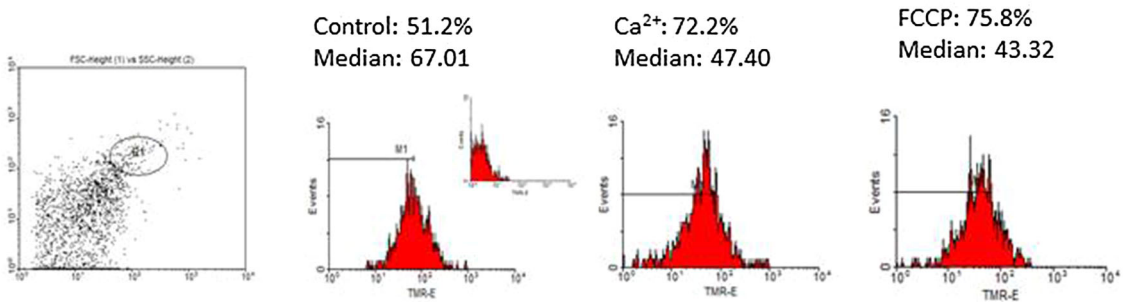


Fig. 3 Mitochondrial membrane potential ($\Delta\psi_m$) measured by changes in TMRE fluorescence in synaptosomes from 3 or 17-months old mice. **a, b** Typical dot-plot of the synaptosomal population and the histograms of gated events (R1) versus relative fluorescence intensity (FL-1) corresponding to different experimental conditions: unloaded, 100 μM Ca²⁺ and 0.5 μM FCCP for 3-months (**a**) or 17-months old mice (**b**). Samples without probe used for

autofluorescence are shown in the *insets*. Each histogram represents a typical experiment, which was performed in triplicate. *Bar* quantification of TMRE fluorescence is shown in panel (c); *bars* represent mean values \pm SEM from 3 independent experiments; **p* < 0.01 significant difference between control (unloaded) and Ca²⁺-incubated samples; #*p* < 0.001, significant difference between control and FCCP-incubated samples

Discussion

During the aging process and age-associated neurodegenerative disorders, mitochondrial dysfunction has emerged as a key factor in the progressive decline of physiological brain function. It is probable that during aging, the brain bioenergetic state could be reflected in brain function

alterations due to the age-related changes in energy production, demand and consumption.

This study was performed in two different subcellular fractions of brain cortex from 3 or 17 months old mice: synaptosomes and non-synaptic mitochondria. Important to note is that brain cortex synaptosomal fraction contains only mitochondria from neuronal origin, whereas non-synaptic

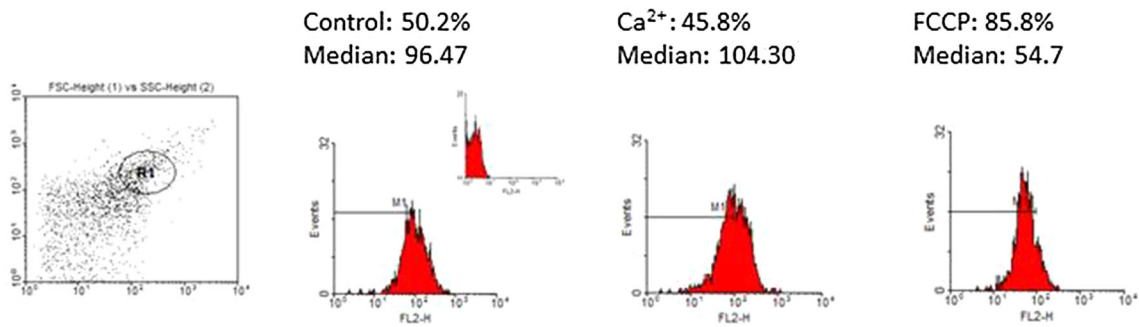
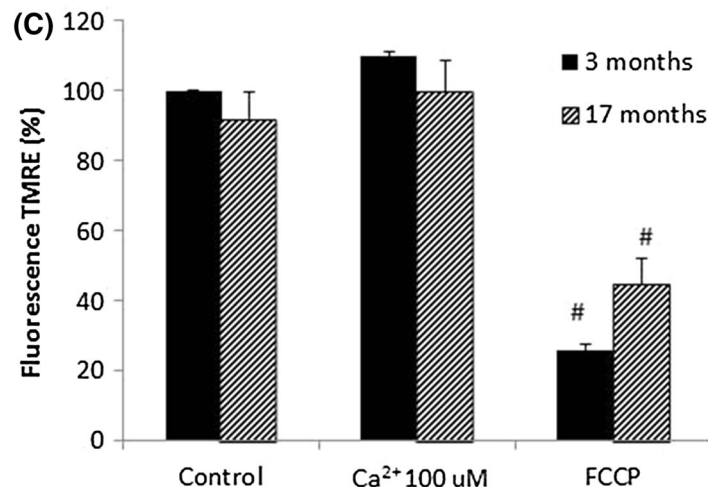
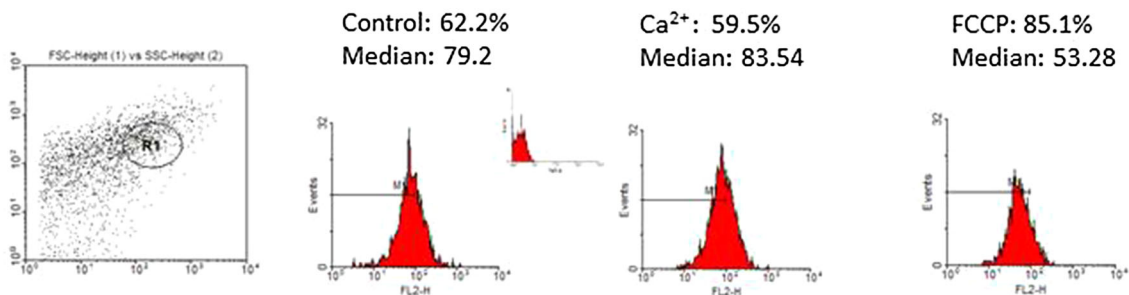
(A) Non-synaptic mitochondria 3 months**(B) Non-synaptic mitochondria 17 months**

Fig. 4 Mitochondrial membrane potential ($\Delta\psi_m$) measured by changes in TMRE fluorescence in non-synaptic mitochondria from 3 or 17-months old mice. **a, b** Typical dot-plot of the mitochondrial population and the histograms of gated events (R1) versus relative fluorescence intensity (FL-1) corresponding to different experimental conditions: unloaded, 100 μM Ca^{2+} and 0.5 μM FCCP for 3-months (**a**) or 17-months old mice (**b**). Samples without probe used for

autofluorescence are shown in the insets. Each histogram represents a typical experiment, which was performed in triplicate. Bar quantification of TMRE fluorescence is shown in panel (c); bars represent mean values \pm SEM from 3 independent experiments; * $p < 0.01$ significant difference between control (unloaded) and Ca^{2+} -incubated samples; # $p < 0.001$, significant difference between control and FCCP-incubated samples

mitochondrial fraction contains mitochondria from glia and astrocytes. Even though non-synaptic mitochondria become from different cell types, there are no important differences in their respiratory function [27]. Particularly, the synaptosomal fraction was characterized by a detailed flow cytometry analysis based on mitochondrial markers: cardiolipin content

and proton gradient, associating both to the particle size. This analysis showed that synaptosomes are among the largest particles. Comparison of the NAO and TMRE histograms for the synaptosomal preparations from young and old mice reveals that the fluorescence intensity in the larger particles is much greater than in the smallest particles.

Table 3 Activity of enzyme complexes of mitochondrial respiratory chain in non-synaptic (NS) mitochondria and in synaptosomal preparations from 3- or 17-months old animals

	Enzymatic activity (nmol/min.mg protein)		
	Complex I–III	Complex II–III	Complex IV
Synaptosomes			
3 months	117 ± 13	26 ± 3	35 ± 4
17 months	131 ± 11	40 ± 4*	57 ± 7*
NS mitochondria			
3 months	124 ± 7	28 ± 2	13 ± 2
17 months	155 ± 11*	23 ± 2	18 ± 2*

Values represent the mean ± SEM

Subcellular fractions were prepared from a pool of 4 mice cerebral cortex. Assays were performed in three independent experiments

* $p < 0.05$

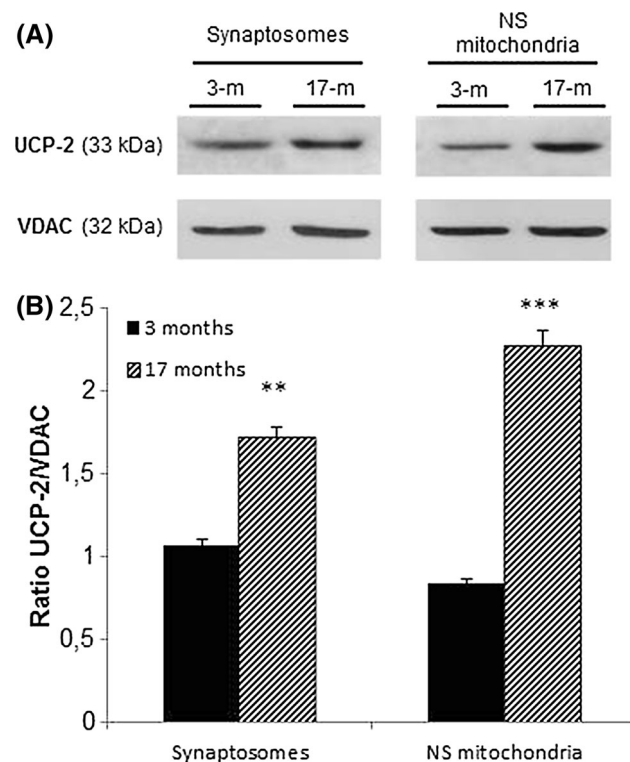


Fig. 5 UCP-2 protein expression in synaptosomes and non-synaptic mitochondria from 3 or 17-months old mice. **a** Western blot analysis of UCP-2 protein expression in synaptosomal and non-synaptic mitochondrial membranes from 3- or 17-months old animals. VDAC was used as loading control. Results are representative of three independent studies. **b** Bars represent UCP-2/VDAC ratio obtained after densitometric analysis. Data (mean ± SEM) are expressed as a % of the control group (set at 100 %). Asterisk correspond to significant differences between 3 and 17-months old animals (** $p < 0.01$, *** $p < 0.001$)

In the present work, oxygen consumption rates were impaired in synaptosomes from 17 months-old mice mainly observed as a decrease in basal respiration and a

tendency to decrease in ATP generation (oligomycin-sensitive mitochondrial respiration), as compared with young animals. The decrease in proton leak (oligomycin-insensitive mitochondrial respiration) in synaptosomes from 17-months old mice could be associated with UCP activity. Aging has been linked to alterations in UCP-2 and -3 gene expression in different tissues [28]. UCP-2 is associated with a mild uncoupling of oxidative phosphorylation; its upregulation can modulate state 4 respiration by decreasing electrochemical proton gradient and thereby reducing the amount of superoxide generation. According to our values of spare respiratory capacity, it seems that the ability of the synaptosome to adjust oxygen consumption in response to intracellular ATP demands was preserved during aging. Our results could be in agreement with recent observations by Stauch et al. [29] showing that while differences can be observed in coupling and electron flow during aging, mitochondrial capacity for substrate oxidation, ATP turnover and proton leak were not found to be significantly different between ages in the synaptic mitochondria. The results obtained for synaptosomal oxygen consumption can be related to the fact that the activity of complexes II–III and IV was 54 and 63 % increased in synaptosomes from 17 months old animals, as compared with young mice.

In addition, the analysis of the respiratory activity of non-synaptic mitochondria in the presence of malate-glutamate substrates showed that state 3 oxygen consumption was not affected by aging. Also, the activity of complex I–III was significantly increased by 25 % in non-synaptic submitochondrial membranes from 17-months old animals, as compared with 3-months old mice. On the contrary, when succinate was added as respiratory substrate, respiratory state 3 rate was decreased by aging in non-synaptic mitochondria, being complex II–III activity unchanged. Thus, it seems that in non-synaptic mitochondria partial energy deficiency during aging could be compensated by the increased activity of complex I–III. Besides, increased activity of cytochrome oxidase (COX) was found in both synaptosomal and non-synaptic mitochondrial fractions. In contrast, some authors have shown a progressive decline in COX activity during aging [30, 31]. However, several reports are in agreement with our results. For instance, protein expression of COX subunits I, II/III, and IV exhibited an age-related increase from 2 months up to 24 months in rat cerebral cortex [32]. Also, increased expression of mitochondrial-encoded genes in complexes I, III, IV, and V of the respiratory chain has been described in 12- and 18-month-old C57BL6 mice compared to 2-month-old mice [33]. Recently, Cuadrado-Tejedor et al. [34] have analyzed the age-related mitochondrial changes in a transgenic model of Alzheimer's disease and found that mitochondrial dysfunction in 7-month-old mice was associated with an increase in COX activity. On the other hand,

Villa et al. (2006, 2009, 2012) showed that the energetic metabolism in the frontal cerebral cortex is poorly affected by aging; respiratory chain complexes activities were not significantly affected during aging, except at 18 months in synaptic mitochondria [35–37].

Synaptic mitochondria and non-synaptic mitochondria respond differentially regarding Ca^{2+} handling [6]. A higher cyclophilin D content in synaptic mitochondria than in non-synaptic mitochondria could contribute to the differential mitochondrial Ca^{2+} buffering capacity, as reported by Naga et al. [38]. This is in accordance with Brown et al. [12] who showed that mitochondria isolated from rat cortical synaptosomes are more prone to undergo MPT in response to Ca^{2+} insult as compared to non-synaptic mitochondria. Also, reactive oxygen species production and mitochondrial membrane potential dissipation induced by 100 and 200 μM Ca^{2+} overload appeared to be higher in synaptic mitochondria than in non-synaptic mitochondria [39].

In the present study, even when no significant statistical differences were found, mitochondrial membrane potential was slightly diminished by aging both in synaptosomes and non-synaptic mitochondria. Accordingly, Choi et al. [20] have reported that synaptosomes from aged mice maintained membrane potential as effectively as those from young mice. However, after calcium overload, mitochondrial membrane potential was significantly decreased in brain cortex synaptosomes from 17-months old mice, but was not affected in synaptosomes from young animals. In non-synaptic mitochondria, membrane potential was rapidly recovered after calcium insult both in young and old animals.

As discussed before, aging has been related with the different gene expression of UCP-2 in various tissues [28]. In our study, an increased UCP-2 protein expression was observed both in synaptosomes and in non-synaptic mitochondria from 17-months old animals as compared with young mice. UCP-2 upregulation would provide a regulatory physiological mechanism by which a mild electron leakage with a slight decrease in energy production could allow the maintenance of low oxygen free radical generation. Our future studies will be conducted to evaluate oxygen free radical generation by synaptosomes and non-synaptic mitochondria during aging.

Conclusions

This study shows the response of synaptosomes and non-synaptic mitochondria to aging. With aging, overall mitochondrial bioenergetics function seems to be preserved in both synaptosomes and non-synaptic mitochondria. However, a decreased mitochondrial membrane potential was observed after calcium overload in synaptosomes from aged mice. UCP-2 upregulation by aging is a possible

mechanism by which mitochondria became resistant to oxidative damage both in synaptosomes and non-synaptic mitochondria.

Acknowledgments This research was supported by Grants from Consejo Nacional de Investigaciones Científicas y Técnicas (CONICET, PIP 112-20110100271), and Universidad de Buenos Aires (UBA, 0020130100255BA), Argentina.

References

- Mattson MP, Gleichmann M, Cheng A (2008) Mitochondria in neuroplasticity and neurological disorders. *Neuron* 60:748–766
- Attwell D, Laughlin SB (2001) An energy budget for signaling in the grey matter of the brain. *J Cereb Blood Flow Metab* 21:1133–1145
- Ly CV, Verstreken P (2006) Mitochondria at the Synapse. *Neuroscientist* 12:291–299
- Knott AB, Perkins G, Schwarzenbacher R, Bossy-Wetzel E (2008) Mitochondrial fragmentation in neurodegeneration. *Nat Rev Neurosci* 9:505–518
- Mac Askill AF, Kittler JT (2010) Control of mitochondrial transport and localization in neurons. *Trends Cell Biol* 20:102–112
- Li Z, Okamoto K, Hayashi Y, Sheng M (2004) The importance of dendritic mitochondria in the morphogenesis and plasticity of spines and synapses. *Cell* 119:873–887
- Hollenbeck PJ, Saxton WM (2005) The axonal transport of mitochondria. *J Cell Sci* 118:5411–5419
- Piccioni F, Pinton P, Simeoni S, Pozzi P, Fascio U, Vismara G, Martini L, Rizzuto R, Poletti A (2002) Androgen receptor with elongated polyglutamine tract forms aggregates that alter axonal trafficking and mitochondrial distribution in motor neuronal processes. *FASEB J* 16:1418–1420
- Rintoul GL, Reynolds IJ (2009) Mitochondrial trafficking and morphology in neuronal injury. *Biochim Biophys Acta* 1802:143–150
- Nicholls DG (2010) Stochastic aspects of transmitter release and bioenergetic dysfunction in isolated nerve terminals. *Biochem Soc Trans* 38:457–459
- Nicholls DG (2003) Bioenergetics and transmitter release in the isolated nerve terminal. *Neurochem Res* 28:1433–1441
- Brown MR, Sullivan PG, Geddes JW (2006) Synaptic mitochondria are more susceptible to Ca^{2+} overload than non synaptic mitochondria. *J Biol Chem* 281:11658–11668
- Sastre J, Pallardó FV, García de la Asunción J, Viña J (2000) Mitochondria, oxidative stress and aging. *Free Radic Res* 32:189–198
- Reddy PH, Beal MF (2008) Amyloid beta, mitochondrial dysfunction and synaptic damage: implications for cognitive decline in aging and Alzheimer's disease. *Trends Mol Med* 14:45–53
- Lores-Arnaiz S, Bustamante J (2011) Age-related alterations in mitochondrial physiological parameters and nitric oxide production in synaptic and non-synaptic brain cortex mitochondria. *Neuroscience* 188:117–124
- Clark JB, Nicklas WJ (1970) The metabolism of rat brain mitochondria Preparation and characterization. *J Biol Chem* 245:4724–4731
- de Lores Rodríguez, Arnaiz G, Girardi E (1977) The increase in respiratory capacity of brain subcellular fractions after the administration of the convulsant 3-mercaptopropionic acid. *Life Sci* 21:637–646
- Lores-Arnaiz S, D'Amico G, Czerniczyniec A, Bustamante J, Boveris A (2004) Brain mitochondrial nitric oxide synthase: in vitro and in vivo inhibition by chlorpromazine. *Arch Biochem Biophys* 430:170–177

19. Lowry OH, Rosebrough NJ, Farr AL, Randall RJ (1951) Protein measurement with the Folin phenol reagent. *J Biol Chem* 193:265–275
20. Choi SW, Gerencser AA, Lee DW, Rajagopalan S, Nicholls DG, Andersen JK, Brand MD (2011) Intrinsic bioenergetic properties and stress sensitivity of dopaminergic synaptosomes. *J Neurosci* 31:4524–4534
21. Estabrook R (1967) Mitochondrial respiratory control and the polarographic measurement of ADP: O ratios. *Methods Enzymol* 10:41–47
22. Petit JM, Huet O, Gallet PF, Maftah A, Ratinaud MH, Julien R (1994) Direct analysis and significance of cardiolipin transverse distribution in mitochondrial inner membranes. *Eur J Biochem* 220:871–879
23. Lores-Arnaiz S, Lores Arnaiz MR, Czerniczyniec A, Bustamante J (2010) Mitochondrial function and nitric oxide production in hippocampus and cerebral cortex of rats exposed to enriched environment. *Brain Res* 1319:44–53
24. Yonetani T (1967) Cytochrome oxidase: beef heart. *Methods Enzymol* 10:332–335
25. Klingenberg M (1999) Uncoupling protein—a useful energy dissipater. *J Bioenerg Biomembr* 31:419–430
26. Gyls KH, Fein JA, Cole GM (2000) Quantitative characterization of crude synaptosomal fraction (P-2) components by flow cytometry. *J Neurosci Res* 61:186–192
27. Hamberger A, Blomstrand C, Lehninger AL (1970) Comparative studies on mitochondria isolated from neuron-enriched and glia-enriched fractions of rabbit and beef brain. *J Cell Biol* 45:221–234
28. Barazzoni R, Nair KS (2001) Changes in uncoupling protein-2 and -3 expression in aging rat skeletal muscle, liver, and heart. *Am J Physiol Endocrinol Metab* 280:E413–E419
29. Stauch KL, Purnell PR, Fox HS (2014) Aging synaptic mitochondria exhibit dynamic proteomic changes while maintaining bioenergetic function. *Aging (Albany NY)* 6:320–334
30. Navarro A, Gomez C, Lopez-Cepero JM, Boveris A (2004) Beneficial effects of moderate exercise on mice aging: survival, behavior, oxidative stress, and mitochondrial electron transfer. *Am J Physiol Regul Integr Comp Physiol* 286:505–511
31. Petrosillo G, De Benedictis V, Ruggiero FM, Paradies G (2013) Decline in cytochrome c oxidase activity in rat-brain mitochondria with aging Role of peroxidized cardiolipin and beneficial effect of melatonin. *J Bioenerg Biomembr* 45:431–440
32. Nicoletti VG, Tendi EA, Lalicata C, Reale S, Costa A, Villa RF, Ragusa N, Giuffrida Stella AM (1995) Changes of mitochondrial cytochrome c oxidase and FoF1 ATP synthase subunits in rat cerebral cortex during aging. *Neurochem Res* 20:1465–1470
33. Manczak M, Jung Y, Park BS, Partovi D, Reddy PH (2005) Time-course of mitochondrial gene expressions in mice brains: implications for mitochondrial dysfunction, oxidative damage, and cytochrome c in aging. *J Neurochem* 92:494–504
34. Cuadrado-Tejedor M, Cabodevilla JF, Zamarbide M, Gómez-Isla T, Franco R, Perez-Mediavilla A (2013) Age-related mitochondrial alterations without neuronal loss in the hippocampus of a transgenic model of Alzheimer’s disease. *Curr Alzheimer Res* 10:390–405
35. Villa RF, Gorini A, Hoyer S (2006) Differentiated effect of aging of Krebs’ cycle, electron transfer complexes and glutamate metabolism of non-synaptic and intra-synaptic mitochondria from cerebral cortex. *J Neural Transm* 113:1659–1670
36. Villa RF, Ferrari F, Gorini A (2012) Energy metabolism of rat cerebral cortex, hypothalamus and hypophysis during ageing. *Neuroscience* 227:55–66
37. Villa RF, Gorini A, Hoyer S (2009) Effect of ageing and ischemia on enzymatic activities linked to Krebs’ cycle, electron transfer chain, glutamate and amino acids metabolism of “free” and intra synaptic mitochondria of cerebral cortex. *Neurochem Res* 34:2102–2116
38. Naga KK, Sullivan PG, Geddes JW (2007) High cyclophilin D content of synaptic mitochondria results in increased vulnerability to permeability transition. *J Neurosci* 27:7469–7475
39. Yarana C, Sanit J, Chattipakorn N, Chattipakorn S (2012) Synaptic and non synaptic mitochondria demonstrate a different degree of calcium-induced mitochondrial dysfunction. *Life Sci* 90:808–814